

Contract No:

This document was prepared in conjunction with work accomplished under Contract No. DE-AC09-08SR22470 with the U.S. Department of Energy (DOE) Office of Environmental Management (EM).

Disclaimer:

This work was prepared under an agreement with and funded by the U.S. Government. Neither the U. S. Government or its employees, nor any of its contractors, subcontractors or their employees, makes any express or implied:

- 1) warranty or assumes any legal liability for the accuracy, completeness, or for the use or results of such use of any information, product, or process disclosed; or
- 2) representation that such use or results of such use would not infringe privately owned rights; or
- 3) endorsement or recommendation of any specifically identified commercial product, process, or service.

Any views and opinions of authors expressed in this work do not necessarily state or reflect those of the United States Government, or its contractors, or subcontractors.

We put science to work.™



**Savannah River
National Laboratory™**

OPERATED BY SAVANNAH RIVER NUCLEAR SOLUTIONS

A U.S. DEPARTMENT OF ENERGY NATIONAL LABORATORY • SAVANNAH RIVER SITE • AIKEN, SC

ANNUAL REPORT, FALL 2016: ALTERNATIVE CHEMICAL CLEANING OF RADIOACTIVE HIGH LEVEL WASTE TANKS- CORROSION TEST RESULTS

R. B. Wyrwas

September 2016

SRNL-STI-2016-00465

SRNL.DOE.GOV

DISCLAIMER

This work was prepared under an agreement with and funded by the U.S. Government. Neither the U.S. Government or its employees, nor any of its contractors, subcontractors or their employees, makes any express or implied:

1. warranty or assumes any legal liability for the accuracy, completeness, or for the use or results of such use of any information, product, or process disclosed; or
2. representation that such use or results of such use would not infringe privately owned rights; or
3. endorsement or recommendation of any specifically identified commercial product, process, or service.

Any views and opinions of authors expressed in this work do not necessarily state or reflect those of the United States Government, or its contractors, or subcontractors.

Printed in the United States of America

**Prepared for
U.S. Department of Energy**

Keywords: *enhanced chemical cleaning, corrosion, permanganate, oxalic acid, nitric acid, tank waste heel*

Retention:

**ANNUAL REPORT, FALL 2016: ALTERNATIVE CHEMICAL
CLEANING OF RADIOACTIVE HIGH LEVEL WASTE TANKS-
CORROSION TEST RESULTS**

R. B. Wyrwas

September 2016



OPERATED BY SAVANNAH RIVER NUCLEAR SOLUTIONS

Prepared for the U.S. Department of Energy under
contract number DE-AC09-08SR22470.

ACKNOWLEDGEMENTS

A special acknowledgement to Matthew Van Swol who performed a majority of the laboratory testing for this report.

Table of Contents

1	Executive Summary	1
2	Background	2
3	Experimental	3
3.1	Test Materials.....	3
3.2	Solutions	3
3.2.1	Permanganate Test Solutions.....	3
3.3	Test setup	4
3.3.1	Planned Interval Tests.....	4
3.3.2	Electrochemical Testing.....	5
3.4	Test Procedure	11
3.5	Post-Test Characterization of Coupons.....	11
3.6	Data Analysis	12
4	Results and Discussion	12
4.1	Task 1 Planned Interval Testing.....	12
4.1.1	Passive coupon data	12
4.1.2	Discussion	13
4.2	Task 2: Electrochemical Corrosion Testing of 304L Stainless Steel with Sodium Permanganate Cleaning Solutions with Sludge Simulants.....	15
4.2.1	Open Circuit Potential (OCP) Measurement.....	16
4.2.2	LPR and CPP results.....	17
4.2.3	Cathodic polarization testing.	19
5	Conclusions.....	20
6	References.....	21

List of Figures

Figure 3-1.	Pourbaix Diagram for water.....	7
Figure 3-2.	Example CPP curve.....	9
Figure 3-3.	Cathodic region of a CPP curve showing the empirically determined E_h	10
Figure 4-1.	Corrosion Rates for Carbon Steel in Acidic Permanganate.	15
Figure 4-2.	Two-hour Open Circuit Measurements for Stainless Steel Exposed to Acidic Permanganate and Caustic Permanganate. Dashed lines represent the respective temperatures with sludge simulant present.....	16
Figure 4-3.	CPP Scan of Caustic permanganate at 30°C.....	18
Figure 4-4.	CPP Scan of Caustic Permanganate with Sludge at 30°C.....	18

Figure 4-5. CPP Scan of Caustic Permanganate with Sludge at 70°C..... 19
 Figure B-6-1. Cyclic Potentiodynamic Polarization Curve of Caustic Permanganate at 30°C. 1
 Figure B-6-2. Cyclic Potentiodynamic Polarization Curve of Caustic Permanganate at 50°C. 1
 Figure B-6-3. Cyclic Potentiodynamic Polarization Curve of Caustic Permanganate at 75°C. 2
 Figure B-6-4. Cyclic Potentiodynamic Polarization Curve of Caustic Permanganate with Sludge at 30°C. 3
 Figure B-6-5. Cyclic Potentiodynamic Polarization Curve of Caustic Permanganate with Sludge at 50°C. 3
 Figure B-6-6. Cyclic Potentiodynamic Polarization Curve of Caustic Permanganate with Sludge at 75°C. 4
 Figure B-6-7. Cyclic Potentiodynamic Polarization Curve of Caustic Permanganate with Sludge at 75°C. 4
 Figure B-6-8. Cyclic Potentiodynamic Polarization Curve of Acidic Permanganate at 30°C. 5
 Figure B-6-9. Cyclic Potentiodynamic Polarization Curve of Acidic Permanganate at 50°C. 5
 Figure B-6-10. Cyclic Potentiodynamic Polarization Curve of Acidic Permanganate at 75°C. 6
 Figure B-6-11. Cyclic Potentiodynamic Polarization Curve of Acidic Permanganate with Sludge at 30°C.6
 Figure B-6-12. Cyclic Potentiodynamic Polarization Curve of Acidic Permanganate with Sludge at 50°C.7
 Figure B-6-13. Cyclic Potentiodynamic Polarization Curve of Acidic Permanganate with Sludge at 75°C.8
 Figure B-6-14. Cyclic Potentiodynamic Polarization Curve of Acidic Permanganate with Sludge at 75°C.8

List of Tables

Table 1. Planned Interval Coupon Test with NA/OA Chemical Cleaning Solution..... 5
 Table 2. Test Matrix for Electrochemical Testing 6
 Table 3. Corrosion Rates for A285 Carbon Steel in Caustic Permanganate Sludge Solution (mpy) 12
 Table 4. Corrosion Rates for A285 Carbon Steel in Acidic Permanganate Sludge Solution 12
 Table 5. Corrosion Rates for 304L Stainless Steel in Caustic Permanganate Sludge Solution 13
 Table 6. Corrosion Rates for 304L Stainless Steel in Acidic Permanganate Sludge Solution..... 13
 Table 7. Change in Environment Corrosiveness and Alloy Corrodibility Determined by the Coupon Interval Tests..... 13
 Table 8. Summary of the Electrochemical Test Results for Open Circuit Potential, Linear Polarization Resistance, and Cyclic Potentiodynamic Polarization Tests..... 17
 Table 9. Cathodic Polarization Results for Caustic Permanganate and Acid Permanganate with and without Sludge Simulant..... 20

Abbreviations

AP	Acidic Permanganate, solution
ASTM	American Society of Testing and Materials
BOAC	Bulk oxalic acid cleaning
CLP	Cathodic linear polarization
CPP	Cyclic potentiodynamic polarization
CP	Caustic Permanganate, solution
DOE	Department of Energy
EM	Environmental Management
HLW	High level waste
HM	H-Modified; The enriched uranium process that recovers plutonium and

	enriched uranium from uranium-aluminum fuel
LPR	Linear polarization resistance
LTAD	Low Temperature Aluminum Dissolution
MPY	mils per year
NA	Nitric acid
OA	Oxalic acid
OCP	Open circuit potential
PAR	Princeton Applied Research
PUREX	Plutonium Uranium Reduction Extraction
SEM	Scanning Electron Microscope
SRNL	Savannah River National Lab
SRS	Savannah River Site

1 Executive Summary

The testing presented in this report is in support of the investigation of the Alternative Chemical Cleaning program to aid in developing strategies and technologies to chemically clean radioactive High Level Waste tanks prior to tank closure. The data and conclusions presented here were the examination of the corrosion rates of A285 carbon steel and 304L stainless steel exposed to two proposed chemical cleaning solutions: acidic permanganate (0.18 M nitric acid and 0.05M sodium permanganate) and caustic permanganate. (10 M sodium hydroxide and 0.05M sodium permanganate). These solutions have been proposed as a chemical cleaning solution for the retrieval of actinides in the sludge in the waste tanks and were tested with both HM and PUREX sludge simulants at a 20:1 ratio.

The corrosion rates determined from passive coupons testing for the A285 carbon steel exposed to the PUREX sludge was found to be as high as 70 MPY at 25°C and 125 MPY at 50°C in the acidic permanganate. Previous testing⁶, show the corrosion rate determined by electrochemical methods to be about 3 MPY at room temperature (about 22°C). The passive coupons displayed signs of general corrosion and pitting corrosion with pits as wide as 2-6 mm and about 1mm deep. There were only 1 or 2 major pits on the coupons that have a surface area of 5.42 in². The large pits could undoubtedly be responsible for the biased corrosion rates in the passive coupon tests. The presence of localized corrosion agrees with the electrochemical data that displayed a positive hysteresis. The corrosion rate was observed to decrease of the testing period at 50°C and remained constant at 25°C.

The corrosion rates determined from passive coupon testing in the caustic permanganate were much lower than the acidic case at about 0.03 MPY at 25°C and 0.24 MPY at 50°C. The corrosion rates measured by electrochemical methods were as high as 3.8 MPY at room temperature. The surface of the passive coupons changed color from a bright polished silver to a metallic gray. Scanning electron microscopy (SEM) with energy dispersed x-ray spectroscopy (EDX) was performed to screen for elemental composition. Manganese was found to have precipitated on to the surface. The surface change presumably would be due to oxidation that would passivate the surface.

The corrosion behavior of 304L stainless steel in the cleaning solutions with the sludge was also studied using passive coupon testing at 25°C and 50°C. The corrosion rates were very low in both the acid and caustic permanganate with the highest rate being 0.037 MPY. The coupons that were exposed to the caustic permanganate solution turned a golden straw color during the testing. SEM/EDX observations showed that these coupons had deposits of aluminum and manganese. The coupons did not have any observable signs of pitting.

Electrochemical tests were conducted on 304L stainless steel with cleaning solutions contacted with the HM sludge at a 20:1 ratio at temperatures of 30°C, 50°C, and 75°C. The electrochemical tests were used to determine the corrosion rate, propensity for localized corrosion, and the likelihood of hydrogen evolution. The highest corrosion rates were around 35 MPY at 75°C in the caustic permanganate solution which was much higher than the corrosion rates for the passive coupon tests. However, the electrochemical tests can over estimate corrosion rates since the measurement is of the instantaneous measurement. In the passive coupon tests, the coupons changed color resulting in metal deposited on to the surface which may have passivated the steel against corrosion. However, with the sludge present there could be other reactions taking place at the surface of the electrode that contribute to the current, but are

not directly related to the oxidation of the stainless steel. The electrochemical tests did not indicate hydrogen evolution was likely in either the caustic or acidic permanganate due to the high noble potential of the stainless steel in the environments.

2 Background

The U. S. Department of Energy (DOE) Office of Environmental Management (EM) has tasked the Savannah River National Laboratory (SRNL) with developing alternative strategies and technologies to chemically clean High Level Waste (HLW) tanks prior to tank closure.¹ Two tank cleaning technologies have already been implemented at the Savannah River Site (SRS): Low Temperature Aluminum Dissolution (LTAD) and Bulk Oxalic Acid Cleaning (BOAC). Recent chemical cleaning efforts on SRS Tank 12 were very successful with regard to bulk sludge heel (especially for Al, Fe, and U phases) and beta/gamma radionuclide removal.² The Tank 12 cleaning strategy utilized the following processing sequence: LTAD, washing, BOAC, and neutralization. Although chemical cleaning using these technologies has been shown to be effective, no disposition path has been identified for oxalate, and insoluble oxalate salts are accumulating within the SRS tank farm and waste processing facilities (e.g., evaporators, etc.).³ Extensive sludge washing that can result in water additions to the tank farm is also required to remove moderately soluble sodium oxalate salts prior to sludge vitrification in the SRS Defense Waste Processing Facility (DWPF). As a result, oxalate additions to the tank farm need to be minimized by the use of supplementary acids to assist sludge removal in OA or the use of other cleaning reagents or processing strategies. Alternatively, methods or strategies to destroy or permanently dispose of the oxalate solids require development.

Past SRNL testing⁴⁻⁶ revealed the importance of pH control for BOAC, recommended the use of a supplementary acid (i.e., dilute HNO₃) with dilute OA to minimize oxalate additions,⁶ and indicated that marginal corrosion rates would be observed with these acid mixtures.⁸ The heel pH was maintained to near the ideal value for sludge dissolution during BOAC (~pH 2) in SRS Tank 12, but a supplementary acid was not utilized. More recent waste simulant studies, have confirmed that manageable carbon steel corrosion rates are observed with mixtures of dilute oxalic and nitric acids.⁹ Separate studies have shown that utilization of this acid mixture as well as pure dilute nitric acid can result in effective dissolution of non-radioactive sludge simulant components with significantly reduced oxalate additions relative to the baseline BOAC treatment.¹⁰ A new cleaning approach was also evaluated with radioactive sludge simulants for the targeted removal of actinide elements which are primary drivers for SRS Tank Closure Performance Assessments.

Although chemical cleaning methods used to date have been implemented in SRS tanks, Hanford HLW tanks may ultimately require cleaning as well. It is believed that SRS cleaning methods could be utilized in some Hanford tanks. However, Hanford waste is more complex and diverse than SRS waste. Retrieval of Hanford HLW tank heels will likely require additional cleaning reagents and methods. The presence of complexants in Hanford waste may allow for the use of a more diverse group of cleaning reagents than are required or allowed for SRS waste.

The Alternative Chemical Cleaning program is divided into the following three primary activities:

- Additional Corrosion Evaluations

- Real Waste Testing
- Scoping Studies to Identify Potential Cleaning Reagents for Hanford HLW Tank Heels

Completion of these activities should validate the current proposed strategy (i.e., dilute oxalic/nitric acid mixtures) for optimized retrieval of SRS waste tank heels and allow for comparison of this method to the baseline BOAC cleaning method using actual waste samples. Additional corrosion evaluations will include final testing required in order to make recommendations regarding the general use of oxalic/nitric acid mixtures for tank heel chemical cleaning. In addition, corrosion evaluations of the permanganate-based actinide removal methodologies will be conducted to further develop a technical basis in regard to the use of these cleaning reagents in the tank farm. Preliminary electrochemical studies indicated surprisingly low carbon steel corrosivity. Solubility evaluations of permanganate-based methods for the retrieval of actinide species from actual sludge samples should determine the feasibility of utilizing this technique for the removal of the primary remaining problematic radionuclides from HLW tank heels. Unique Hanford waste phases will be identified for solubility evaluations and, preliminary laboratory testing will be conducted as the next phase of this program if the scope of work is increased.

3 Experimental

3.1 Test Materials

American Society of Testing and Materials (ASTM) A285 carbon steel materials were utilized for the corrosion tests. The Type I and II SRS waste tanks, which are the initial tank groups targeted for chemical cleaning and closure, were constructed of A285 carbon steel. Immersion test coupons were sectioned from a plate of A285 material supplied by Metal Samples Company™ (Munford, AL). The coupons were polished to a 600 grit finish to provide a uniform, reproducible surface prior to testing. This surface preparation was utilized in the previous corrosion tests for the same purposes.⁸

The test material, 304L stainless steel, was also used for the corrosion tests. SRS tank farm transfer lines and ventilation system materials were constructed of 304L stainless steel. Immersion coupons were sectioned from a plate of 304L material also supplied by Metal Samples Company™. The coupons were polished to a 600 grit finish to provide a uniform, reproducible surface prior to testing.

3.2 Solutions

3.2.1 Permanganate Test Solutions.

Caustic permanganate (CP) and acidic permanganate (AP) at the following solution compositions were utilized for the tests.

- 1) 10 M sodium hydroxide / 0.05 M sodium permanganate
- 2) 0.18 M nitric acid / 0.05 M sodium permanganate

In addition to tests in these solutions, tests were performed in these solutions combined with the PUREX and HM simulants developed by Eibling.¹¹ These conditions will simulate the proposed chemical cleaning process. Previous testing with oxalic acid has shown that the presence of the simulated sludge solids, and the associated interstitial liquid, affects the corrosion behavior of the carbon steel.^{6,9} The liquid to solid phase ratios used for testing were 20:1. The designation for caustic permanganate with

sludge (CPS) and acid permanganate with sludge (APS) may be used in the data tables and figures. Tests were conducted at the temperatures specified for each task with temperature monitoring. In order to obtain better dissolution of the solids, the waste is typically agitated by pumps. Previous laboratory testing has also suggested that agitation results in higher general corrosion rates. Therefore, the simulants were agitated during the testing.⁹

3.3 Test setup

There are two tasks reported in this report. Planned interval tests use the corrosion rates for a given testing period to determine the material performance over a 30-day experiment. Electrochemical corrosion testing was performed using 304L stainless steel to determine the corrosivity and to investigate the probability of hydrogen evolution.

3.3.1 Planned Interval Tests

Passive coupon testing was performed at 25°C and 50°C using gravimetric methods to determine the corrosion rates for both the A285 carbon steel and the 304L stainless steel. Changes in the solution corrosivity (i.e., aggressiveness of the environment) and alloy corrodibility (i.e., corrosion susceptibility, passive layer formation and/or degradation, etc.) were determined by employing a planned interval testing schedule. The interval schedule for the test is summarized in Table 1. In these tests, the waste simulants are contacted with the CP and AP cleaning reagents for a period of four weeks and steel coupons are immersed in this slurry for the intervals indicated. A minimum set of 3 flat, rectangular coupons (2.54 cm x 5.08 cm x 0.60 cm) with a surface area of 34.95 cm² (5.42 in²) is initially exposed to the corrosive environment of interest. Coupon A1 was removed after 1 week of exposure, coupon A3 was removed after 3 weeks, and coupon A4 was removed after 4 weeks of exposure. Coupon B, another flat, rectangular coupon, was placed in at 3 weeks and was removed along with Coupon A4 after week 4.

The corrosion rates for A₁, A₃, A₄, and B are obtained by determining the mass lost during the test and determining the corrosion rate accordingly. A₂ is the calculated difference in the corrosion rates between Coupon numbers A₄ and A₃. When B=A₁ the corrosivity of the environment has not changed after 3 weeks of exposure. On the other hand, if B < A₁ the corrosivity has decreased or if B > A₁ it has increased. Corrosion rate A₂ evaluates the corrodibility of the alloy. When A₂ = B the alloy corrodibility has not changed after 3 weeks of exposure. In contrast, if A₂ < B the corrodibility has decreased, and when A₂ > B it has increased.

Table 1. Planned Interval Coupon Test with Chemical Cleaning Solution

Coupon					
	A1				
No.1					
		A3		A2	
No. 2					
				A4	
No. 3					
				B	
No. 4					
	1	2	3	4	
	Time(weeks)				
Criteria	Environment Corrosiveness		Criteria	Alloy Corrodibility	
B = A1	Unchanged		A2 = B	Unchanged	
B < A1	Decreased		A2 < B	Decreased	
B > A1	Increased		A2 > B	Increased	

3.3.2 Electrochemical Testing

The electrochemical tests were conducted in a cell similar to the Princeton Applied Research (PAR) corrosion cell using a flat square electrode (1.905 cm x 1.905 cm) of 304L stainless steel embedded in epoxy with a flat exposed surface area of 3.629 cm². The electrode was connected by a piece 22 gauge wire that was spot welded to the sample before embedding. The sample was then polished to a 600-grit finish. After each set of measurements, the sample was resurfaced by wet polishing first with 240-grit sand paper, then 600-grit paper.

Four electrochemical tests were performed at each condition listed in Table 2. They are:

- 1) monitoring of the open-circuit potential (OCP),
- 2) linear polarization resistance testing (LPR),
- 3) cyclic potentiodynamic polarization testing (CPP), and
- 4) cathodic linear polarization testing (CLP).

Between tests 2 and 3 and tests 3 and 4, the open circuit was monitored for 10 minutes. Before running the CLP test, the electrode was resurfaced. This was done to avoid any impacts from the CPP test.

Previous testing used a sequential testing and resulted in a film over the working electrode after the CLP and the CPP tests were performed.⁶ Since the test solution is very opaque from both the permanganate and the sludge, it is impossible to observe the electrode surface without removing the electrode. Therefore it was chosen to resurface the working electrode prior to the CLP. These tests were conducted with a VMP3 potentiostat. Graphite rods were used as counter electrodes. A luggin bridge filled with 9% sodium nitrate was used with a Ag/AgCl reference electrode to prevent continuous maintenance of reference electrodes and preserve data quality. The tests were measured with respect to the reference potentials.

The OCP reflects a measure of the activity at the metal surface for all oxidation and reduction reactions, i.e., whether it is actively corroding or passive, while the LPR testing will give a direct measure of the instantaneous corrosion rate. The cathodic polarization (CLP) is performed to understand the kinetics of the cathodic reaction, while the cyclic potentiodynamic polarization (CPP) testing was performed separately to reveal any vulnerability to localized corrosion, such as stress corrosion cracking and/or pitting. The open circuit potential was measured during a 10-minute rest period between techniques to monitor for any significant changes to the surface of the sample during testing. These tests provide necessary mechanistic information to support the results of future coupon tests as well as screen for potential process conditions, which may result in lower corrosion rates. The conditions with lower corrosion rates could then be the focus of the coupon tests.

The test matrix in Table 2 outlines the temperature and solution conditions for the electrochemical testing. The sludge simulant used was the HM simulant.¹²

Table 2. Test Matrix for Electrochemical Testing

Test	Sludge Ratio	Solution	Temperature, °C
1	None	CP	30
2	None	CP	50
3	None	CP	75
4	None	AP	30
5	None	AP	50
6	None	AP	75
7	20:1	CP	30
8	20:1	CP	50
9	20:1	CP	75
10	20:1	AP	30
11	20:1	AP	50
12	20:1	AP	75
AP= Acidic Permanganate CP= Caustic Permanganate			

3.3.2.1 Open Circuit Potential

The OCP reflects a measure of the electrochemical activity at the metal surface, i.e. whether it is actively corroding or becoming passive. The test also provides information on the relative stability of the passive film, and whether hydrogen evolution is thermodynamically possible. For these tests, the OCP will be

monitored daily to determine if changes in the passive film or environment may lead to a propensity for hydrogen evolution at any time during the test.

The propensity for hydrogen evolution may be visualized with the Pourbaix diagram for water, which is shown in Figure 3-1. The two diagonal lines, identified as (a) and (b), define the region of stability for water as a function of potential and pH. For potential and pH conditions between lines (a) and (b), water is thermodynamically stable. For any value of potential above line (b), water is thermodynamically unstable and oxygen is liberated, while at any conditions of potential and pH below line (a), water is thermodynamically unstable and hydrogen gas is generated. Therefore, from the measured potential and the pH values, it can be determined if it is thermodynamically possible for the corrosion reaction to generate hydrogen. If the measured OCP value from the test is below line (a), hydrogen evolution is thermodynamically possible.

The equation for line (a) is derived from the Nernst Equation:

$$E_{H_2} = E^\circ - 2.303 \frac{RT}{F} *pH \quad (1)$$

where E_{H_2} is the potential below which hydrogen evolution is thermodynamically stable, E° is the standard potential for hydrogen ($E^\circ = 0.0$ V vs. SHE), R is the ideal gas constant, 8.314 J/mole-K, T is the temperature in K, and F is the Faraday constant, $96,500$ J/equivalent. The potential utilized in the Nernst equation is with reference to the standard hydrogen electrode (SHE). Experimental measurements during these tests were made using a saturated Ag/AgCl reference electrode. To convert the potentials that are referenced to the hydrogen potential to one with reference to the Ag/AgCl, 197 mV are subtracted from E_{H_2} . The potential below which hydrogen evolves can be determined as a function of pH and temperature.

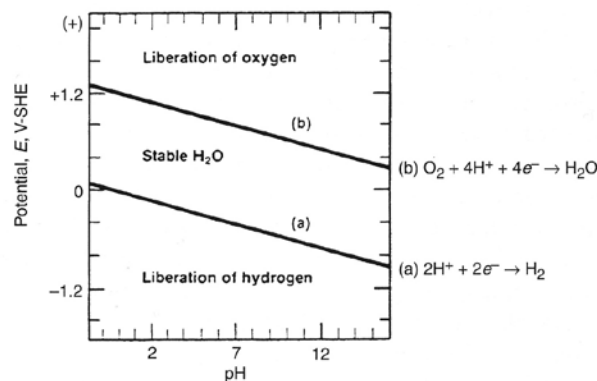


Figure 3-1. Pourbaix Diagram for water.

3.3.2.2 Linear Polarization Resistance

The LPR technique provides a non-destructive, instantaneous estimate of the uniform or general corrosion rate. In contrast, gravimetric (i.e., weight loss) measurements from coupons provide historical or

integrated mass loss information from corrosion that has occurred over some period of time. The ASTM standard practice was utilized to conduct the test.¹³ The technique is based on the observation that when the potential at the metal surface is polarized anodically or cathodically within 15 mV of the OCP, the measured current density at the metal surface increases linearly with potential. The slope of this line is defined as the polarization resistance (R_p). Stern and Geary modified the fundamental equation for electrochemical reaction kinetics, and demonstrated that the relationship between the corrosion current density (i_{corr}) and R_p at the OCP is:

$$i_{\text{corr}} = \frac{\beta_a \beta_c}{2.3(\beta_a + \beta_c)R_p} \quad (2)$$

where β_a and β_c are the anodic and cathodic Tafel slopes, respectively. If the Tafel slopes are unknown, frequently the assumed value for β_a and β_c is 0.120 V/decade. It has been shown experimentally that approximate values for β_a and β_c near 0.1 V/decade give a constant error in calculated corrosion rate of only a factor of two maximum.¹⁴ Such an error is frequently within experimental scatter for in plant corrosion measurements (i.e., typically gravimetric). Therefore, unless the actual slopes are quite different than 0.120 V/decade, the error in the value of i_{corr} is not significant.

Furthermore Stern states that i_{corr} measured by this technique differs from the actual corrosion rate by no more than a factor of two.¹⁵ In a more recent review Mansfield¹⁴ showed from theoretical principles that the error in i_{corr} measurement is likely within $\pm 50\%$ of the actual corrosion rate. Weight loss measurements for corrosion rates are typically reproducible to within 20 to 50%. Therefore, the inherent error in the corrosion rate measurement by either technique is similar.

The corrosion current density is related to the corrosion rate (CR) by the following equation:

$$\text{CR} = 0.13 * \frac{i_{\text{corr}} E_w}{\rho} \quad (3)$$

where i_{corr} is in $\mu\text{A}/\text{cm}^2$, E_w is the equivalent weight of iron (27.9 g/equivalent), and ρ is the density of the metal; for carbon steel 7.86 g/cm^3 , and for stainless steel 7.94 g/cm^3 was used. The corrosion rate is reported in mils (0.001 inches) per year.

3.3.2.3 Cyclic Potentiodynamic Polarization

Cyclic potentiodynamic polarization (CPP) will be the final electrochemical test performed. The CPP test was initiated at a potential approximately 50 mV less than the E_{corr} at a given time. [Note: E_{corr} is the potential at which the rate of the anodic reaction equals the rate of the cathodic reaction. The value of E_{corr} depends on the kinetics of the anodic and cathodic half-cell reactions. For these tests, the value of E_{corr} is very close to the OCP.] A sequentially increasing potential will be applied to the probe at scan rate of 0.167 mV/s. The current response to the change in potential is measured to establish a current-potential relationship. At a potential approximately 1 V above the E_{corr} , the scan is reversed such that a sequentially decreasing potential is applied to the probe at the same scan rate. An example of a CPP curve from these tests is shown in Figure 3-2.

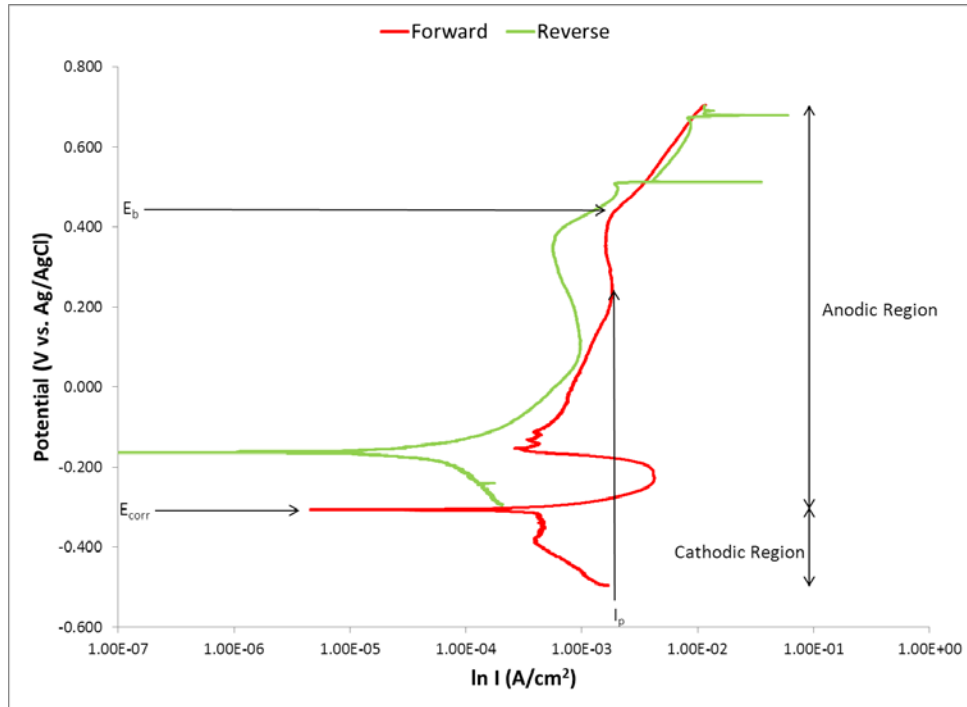


Figure 3-2. Example CPP curve.

The CPP curve will be utilized for three purposes. The first analysis involves the cathodic region of the CPP plot, which extends from E_{corr} to more negative potentials (see Figure 3-2). This region was used to investigate the kinetics of the cathodic electrochemical reaction. From these studies, the propensity for hydrogen may be investigated. At potentials relatively close to the E_{corr} , the relationship between the potential and the current is given by the Tafel expression

$$\eta = \beta \log (i/i_0) \quad (4)$$

where η is the overpotential, defined as $E - E_{\text{corr}}$, in volts; β is the slope of the line on the potential-log current density plot, also known as the cathodic Tafel slope in V/decade; i is the measured current density at the applied potential, E , in A/cm^2 ; and i_0 is the exchange current density, in A/cm^2 , and represents the current density equivalent to the equal forward and reverse reactions at the electrode at equilibrium.

The dominant term controlling the corrosion rate for many metals exposed to non-oxidizing acids, such as oxalic acid, is hydrogen overpotential at cathodic areas of the metal. Hydrogen overpotential is the difference of potential between a cathode at which hydrogen is being evolved, and a hydrogen electrode at equilibrium in the same solution. The rate at which hydrogen evolution occurs depends on the catalytic properties of the electrode surface. For example, a relatively pure iron-based alloy corrodes at a low rate compared to an alloy that contains impurities such as carbon, sulfur and phosphorous, which catalyze the hydrogen reaction.

To determine if hydrogen is the dominant cathodic reaction the following relationship was utilized:

$$\alpha = 2.3 R T / (\beta F) \quad (5)$$

where α is the transfer coefficient, R is the universal gas constant equal to 8.314 J/mole-K, T is the temperature in K, and F is the Faraday constant equal to 96,500 J/equivalent. For iron and steel, α is approximately 0.4 to 0.6 if the hydrogen reaction is occurring at the surface.¹⁶ If α is significantly less than 0.4, this is typical of a cathodic reaction that is diffusion controlled (i.e., β approaching infinite values). That is, the rate of cathodic reaction is dependent upon diffusion of the oxidizer to the electrode surface.

The cathodic region of the scan will be investigated to determine which reactions are possibly dominant. Of particular interest is the potential at which hydrogen evolution appears to be the clearly dominant cathodic reaction. This potential, defined as E_h , is determined empirically from the cathodic region of the CPP plot as shown in Figure 3-3. Below this potential, the slope of the line on the potential-log current density plot is such that α from Equation 5 is approximately 0.4 to 0.6. For potentials at or below this value, hydrogen is the dominant cathodic reaction on the steel surface.

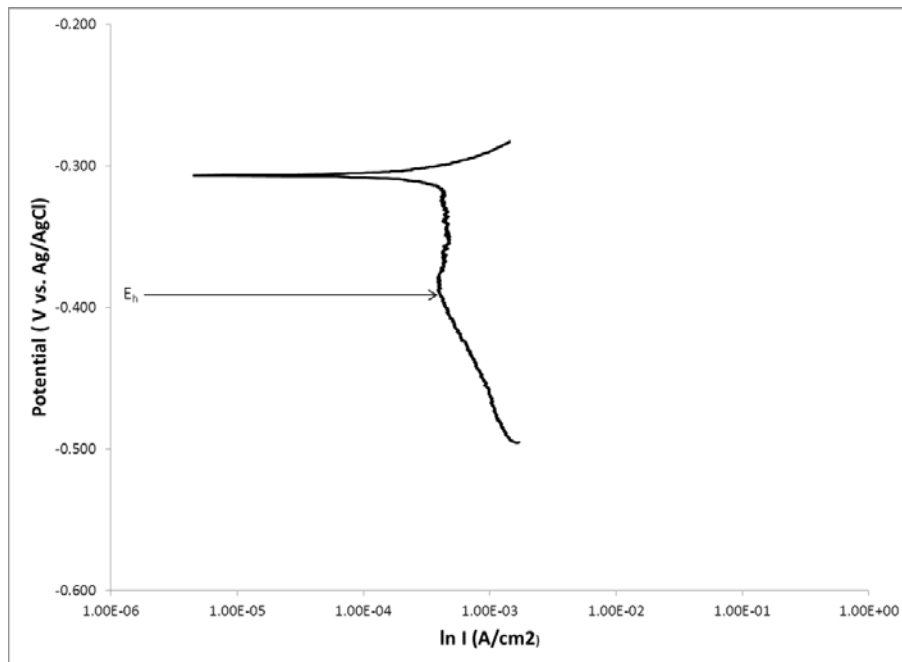


Figure 3-3. Cathodic region of a CPP curve showing the empirically determined E_h .

The anodic region of the CPP curve extends from E_{corr} to the more positive potentials of the forward scan. The current response provides mechanistic information on the metal dissolution or passivation reactions occurring at the metal surface. Current peaks are typically associated with metal dissolution and/or the oxidation of electro-active species in solution at the metal surface. Regions where the current is constant, and possibly low, are associated with passivation of the surface.

Various current responses that occur during the anodic or forward scan have been shown to be indicative of localized corrosion susceptibility. In particular, the breakdown potential, E_b , is the potential where the current increases rapidly with a small change in potential. This change has been correlated with a reduction in the passive nature of the material. The passive to active transition region shown in Figure 3-2 is the region in which the material is susceptible to localized corrosion. The smaller the difference between values of E_{corr} and E_b , the more susceptible the material is to localized corrosion in that environment. The passive current density is also indicative of the protective nature of the oxide film, or in this case the oxalate film. Lower passive current densities are indicative of a more stable protective film.

Data from the reverse scan as well as the forward scan are utilized to determine susceptibility to localized corrosion. If the current density of the reverse scan is greater than that for the forward scan, localized corrosion is likely. This behavior is known as positive hysteresis and indicates that pits have formed and are continuing to propagate. If the current density of the reverse scan is less than that for the forward scan, passive behavior is expected. This behavior is known as negative hysteresis and indicates that the passive film has re-formed on the surface.

3.4 Test Procedure

The electrochemical testing was performed using a Biologic VMP3 potentiostats and EC Lab[®] control and analysis software. The linear polarization tests were done by performing a linear sweep of the potential from -0.25 mV to 0.25 mV with respect to the open circuit potential (OCP) measurement at a scan rate of 0.166 mV/second. The CPP tests were performed by a linear sweep of the potential beginning at -0.250 V with respect to the open circuit potential at a scan rate of 0.166 mV/second to either a current limit (1.0 mA/cm²) or a potential limit of 1.5 V vs. OCP. The CLP test scanned from the OCP to -0.25 V vs. OCP at a rate of 0.166 mV/second.

3.5 Post-Test Characterization of Coupons

After testing, the passive coupons were treated with Clarke's solution to remove the corrosion products and determine the total weight loss due to corrosion processes in the experiment. The coupons were exposed for 3 minutes initially, then successively for 2 minutes. For the coupons that still had a high amount of corrosion products after 7 minutes of exposure, the coupons were exposed at 5-minute intervals. The coupon mass was recorded after each exposure. At the conclusion of the cleaning, the coupons were photographed. The final photographs will be assembled as an appendix to this report.

The corrosion rate was calculated in mils (millinches) per year (MPY) based on the mass loss in accordance with ASTM G 1-03.¹⁷ The method calls to use the following equation:

$$\text{Corrosion Rate} = \frac{K \times W}{A \times T \times \rho}$$

Where, K is a conversion constant, 3.45×10^6 , for MPY, W is the mass loss in grams, A is the surface area in cm², T is the exposure time in hours, and ρ is the density in grams/cm³. The surface area of the corrosion coupons was determined to be 35.9504 cm².

3.6 Data Analysis

The instantaneous corrosion rates were determined from the polarization resistance measurements using EC Lab[®] software. Data was collected and recorded in laboratory notebook SRNL-NB-2014-00037, “Corrosion Testing Experiments,” and electronic notebook i7006-00164, “Corrosion Testing.”

4 Results and Discussion

4.1 Task 1 Planned Interval Testing

4.1.1 Passive coupon data

The corrosion rates are presented in Table 3 thru Table 6 for the caustic permanganate and acidic permanganate solutions with a 20:1 solution to sludge ratio at 25°C and 50°C. The greatest corrosion rates were found for the A285 carbon steel were 124 MPY in the acid permanganate solution at 50°C, nearly double the rate observed at 25°C of 69.1 MPY. The carbon steel in the caustic permanganate showed low corrosion rates with the highest rate observed to be 0.240 MPY in the 50°C test. As expected the general corrosion rates for the 304L were very low, well below 0.1 MPY and did not appear to display localized corrosion such as pitting. A summary of the alloy corrodibility and environment corrosiveness is given in Table 7.

Table 3. Corrosion Rates for A285 Carbon Steel in Caustic Permanganate Sludge Solution (mpy)

Coupon	Time (Hrs)	25°C	50°C
A1	168	0.030	0.240
A2	168	nil	nil
A3	504	0.127	0.098
A4	672	0.071	0.071
B	168	0.052	0.166

Table 4. Corrosion Rates for A285 Carbon Steel in Acidic Permanganate Sludge Solution

Coupon	Time (Hrs)	25°C	50°C
A1	168	69.1	124
A2	168	nil	nil
A3	504	47.2	45.7
A4	672	29.7	37.3
B	168	66.1	21.0

Table 5. Corrosion Rates for 304L Stainless Steel in Caustic Permanganate Sludge Solution

Coupon	Time (Hrs)	25°C	50°C
A1	168	0.037	nil
A2	168	nil	0.079
A3	504	0.017	nil
A4	672	0.004	nil
B	168	nil	nil

Table 6. Corrosion Rates for 304L Stainless Steel in Acidic Permanganate Sludge Solution

Coupon	Time (Hrs)	25°C	50°C
A1	168	0.030	nil
A2	168	0.022	nil
A3	504	nil	nil
A4	672	0.007	nil
B	168	nil	nil

Table 7. Change in Environment Corrosiveness and Alloy Corrodibility Determined by the Coupon Interval Tests

		25°C		50°C	
Test		Environment	Alloy	Environment	Alloy
Acidic	Stainless Steel	Decreased	Increased	Unchanged	Unchanged
	Carbon Steel	Unchanged	Decreased	Decreased	Decreased
Caustic	Stainless Steel	Decreased	Decreased	Increased	Increased
	Carbon Steel	No Change	Decreased	Increased	Decreased

4.1.2 Discussion

The behavior of A285 carbon steel in the acidic permanganate showed the most aggressive corrosion. The coupons showed areas of pitting and had the highest mass loss, which translates to highest corrosion rates in the experiment. The results are displayed graphically in Figure 4-1. The corrosion rate at 50°C was 124 MPY for coupon A1, which was during the first week of the test, but the rate slowed to 21 MPY

for coupon B, which was during the final week indicating the environment became less aggressive. This was not the case for the test at 25°C where the final week corrosion rate was 66 MPY which is about the same as the first week corrosion rate of 69 MPY. The alloy corrodibility decreased at both temperatures which indicates the oxide layer that is formed during the corrosion process passivates the base metal and slows oxidation. This is observed by comparing the calculated A2 corrosion rate to coupon B, A2 is less than B in both cases indicating a decreasing rate as the test progressed. However, the corrosiveness of the environment remained unchanged at 25°C, but decreased during the 50°C test. One artifact of the test that may impact the results is the pitting corrosion that occurred on the coupons. The pitting on the A3 coupon in the acid permanganate at 25°C had a large pit that could have aggressively corroded and given a higher corrosion rate than may be the statistical average. This would require retesting to determine for certain.

In the caustic permanganate, the carbon steel had corrosion rates that were low where the highest rate was 0.127 MPY at 25°C, yet the highest rate was only 0.240 MPY at 50°C. With the corrosion rates being so low, it may be hard to discern the difference in the corrosiveness and corrodibility even though the results are list in Table 7 by definition, more data points should be collected to identify the trend. In addition, some of the coupons appeared to have a gray metallic coating on them. Scanning electron microscopy (SEM) with energy dispersed x-ray spectroscopy (EDX) was performed to screen for elemental composition. Manganese was found to have precipitated on to the surface (results not shown).

The 304L stainless alloy showed very little weight loss at the 4 test conditions, with only the caustic permanganate at 50°C exhibiting a total weight loss of greater than 1 mg. Some of the coupons showed a gain in mass and were a straw or golden color post testing. This increase in mass is indicated by the negative corrosion rates for the stainless steel tests. SEM and EDX were used to screen one coupon. Aluminum and manganese was found to be present on the surface (results not shown). No further investigation was performed on the surfaces.

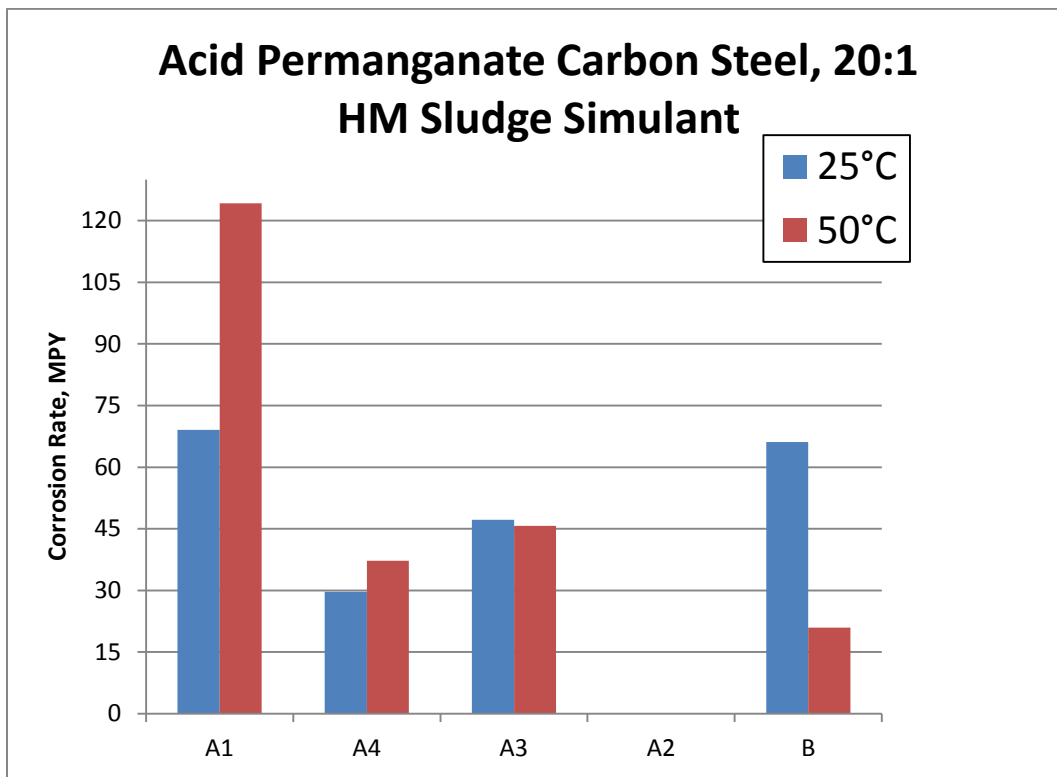


Figure 4-1. Corrosion Rates for Carbon Steel in Acidic Permanganate.

4.2 Task 2: Electrochemical Corrosion Testing of 304L Stainless Steel with Sodium Permanganate Cleaning Solutions with Sludge Simulants

The results from the electrochemical corrosion testing described in section 3.3.2 are presented for 12 tests performed for Table 2 using 304L stainless steel in the caustic permanganate and the acidic permanganate solutions, with and without sludge present at 30°C, 50°C, and 75°C. The electrochemical tests were performed in the following order:

1. Open Circuit Measurement (OCP), 2 hours
2. Linear Polarization scan
3. OCP, 10 mins
4. Cyclic Potentiodynamic Polarization
5. OCP, 10 mins
6. Pause to resurface the coupon
7. OCP, 1 hour
8. Cathodic Linear Polarization

4.2.1 Open Circuit Potential (OCP) Measurement

The OCPs were measured while before and in between the electrochemical tests. Rest periods were used to allow the corrosion potential to equilibrate before a test. The initial OCPs are given in Table 8 and are presented in Figure 4-2 for the 12 tests in Table 2.

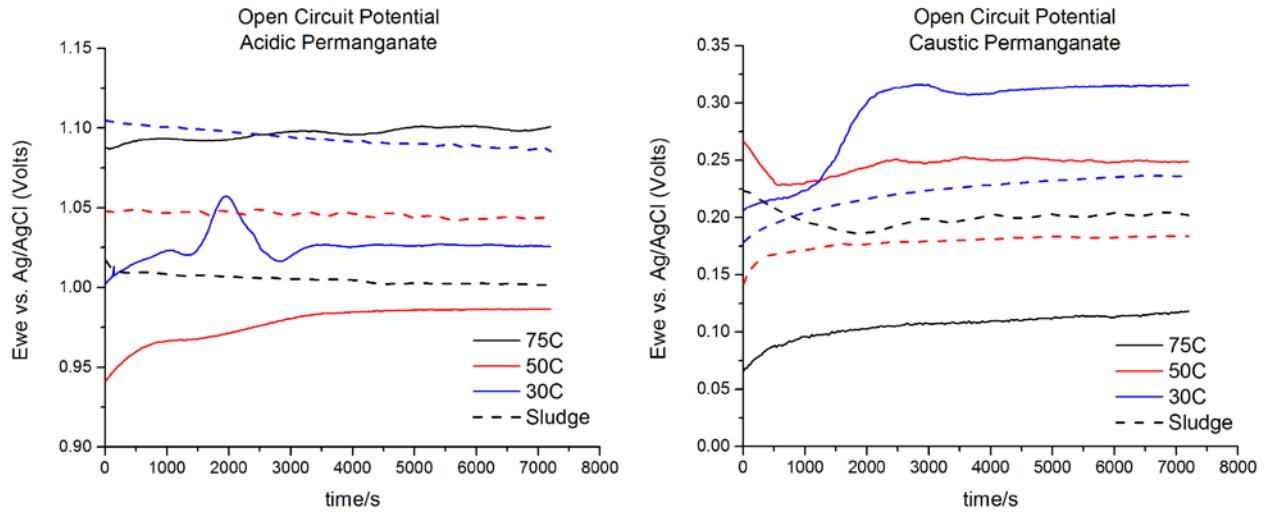


Figure 4-2. Two-hour Open Circuit Measurements for Stainless Steel Exposed to Acidic Permanganate and Caustic Permanganate. Dashed lines represent the respective temperatures with sludge simulant present.

Table 8. Summary of the Electrochemical Test Results for Open Circuit Potential, Linear Polarization Resistance, and Cyclic Potentiodynamic Polarization Tests.

Test	Solution	Temperature, °C	OCP, mV	Corrosion Rate (MPY)	CPP	
					Hysteresis	Notes:
				<i>LPR</i>		
1	CP	30	315	5.18	slight Positive	E_{rp} near E_{corr}
2	CP	50	249	1.76	None	
3	CP	75	118	12.9	slight Positive	E_{rp} near E_{corr}
4	AP	30	1026	7.97	None	
5	AP	50	986	2.00	None	
6	AP	75	1098	0.24	Positive	
With HM Sludge Simulant diluted to 20:1 by solution						
7	CP	30	236	5.82	Negative	$E_{rp} > E_{corr}$
8	CP	50	184	1.15	slight Negative	
9	CP	75	203	34.8	Positive	$E_{rp} < E_{corr}$
9dup	CP	75	179	16.7	Positive	E_{rp} near E_{corr}
10	AP	30	1087	8.21	slight Negative	
11	AP	50	1044	9.35	slight Positive	
12	AP	75	1003	4.33	slight Negative	$E_{rp} > E_{corr}$
12dup	AP	75	2680(?)	13.8	None	

4.2.2 LPR and CPP results.

Table 8 gives the general corrosion rates for the LPR tests on the 12 tests in the test matrix in Table 2. The corrosion rate was calculated from a polarization resistance fit discussed in Section 3.3.2.2. The corrosion rates from the LPR curves were much higher than the corrosion rates in the gravimetric tests discussed in section 4.1. The CPP curves also indicate localized corrosion is possible at the higher temperatures.

Figure 4-3 shows the response for caustic permanganate at 30°C. The forward scan does not display a passive current which is indicative of active general corrosion and the reverse current has a slight positive hysteresis. In the presence of sludge, as shown in Figure 4-4, the CPP curve shows a less active response with a slight passive current and a negative hysteresis. This passivity is more prominent at 50°C. However, at 75°C, the CPP curve indicated localized corrosion as observed in Figure 4-5. In the acidic permanganate, the CPP shows a small region of passivation with a slight positive hysteresis that could be an indication of localized corrosion, with the sludge present, the hysteresis becomes negative.

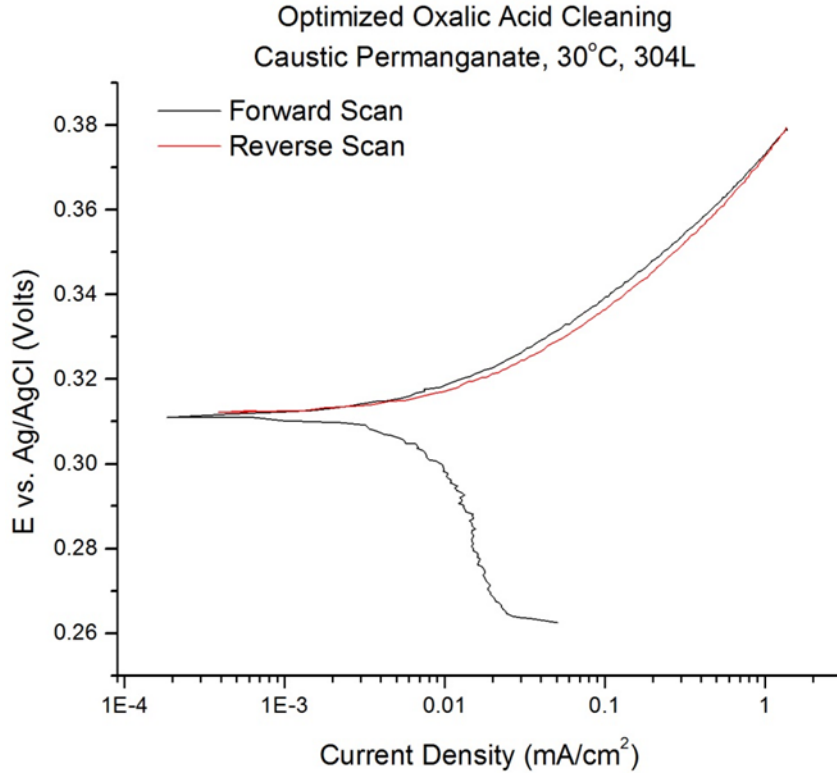


Figure 4-3. CPP Scan of Caustic permanganate at 30°C

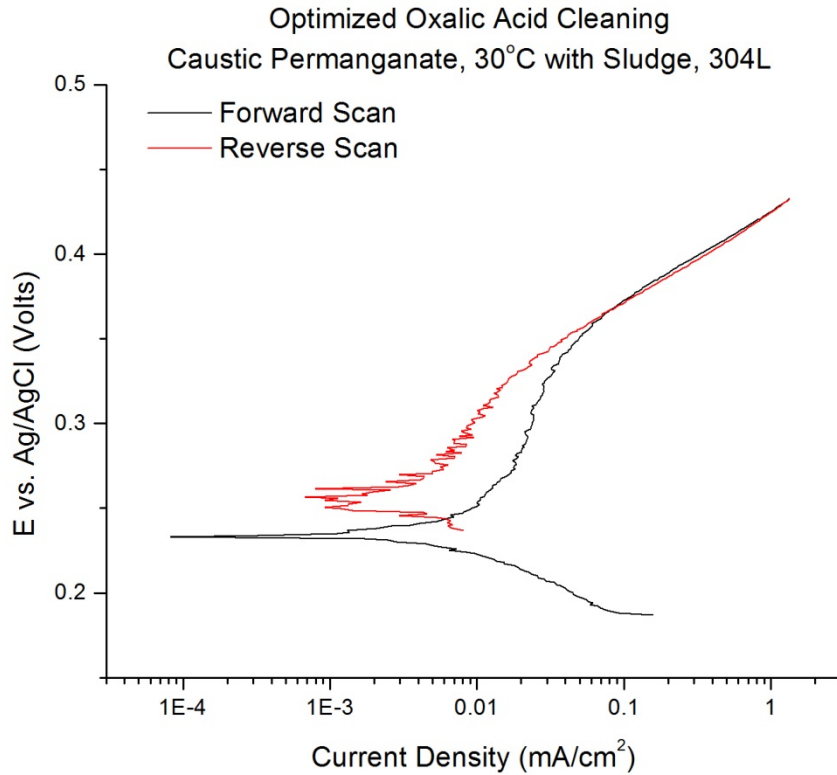


Figure 4-4. CPP Scan of Caustic Permanganate with Sludge at 30°C.

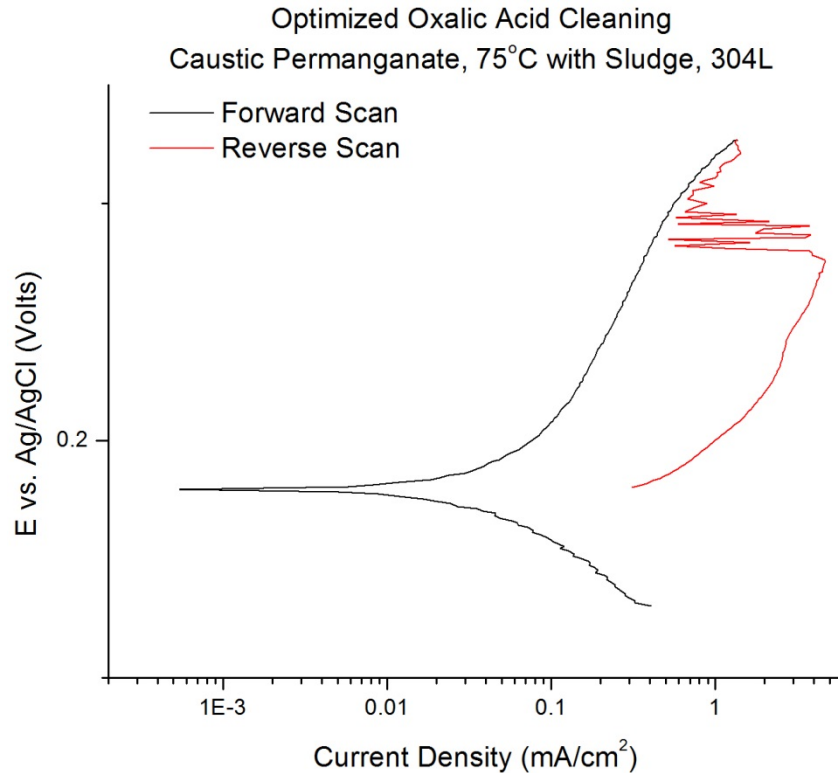


Figure 4-5. CPP Scan of Caustic Permanganate with Sludge at 70°C.

4.2.3 Cathodic linear polarization testing.

Table 9 gives the results of the cathodic polarization testing results. The purpose of this testing is to determine the kinetics of the cathodic reaction and if hydrogen will be evolved as an active process when the acid interacts with the waste. In order for hydrogen evolution to occur, the value α must be within a range of 0.4 to 0.6 as discussed in Section 3.3.2.3 and below the potential for the hydrogen reduction reaction. In the basic conditions the open circuit potential is more noble than the potential for hydrogen evolution. In all cases, permanganate reduction or oxygen evolution are the more likely candidates for the cathodic reaction.

Table 9. Cathodic Linear Polarization Results for Caustic Permanganate and Acid Permanganate with and without Sludge Simulant.

Test	Solution	Temperature, °C	β (mV/decade)	i_o (Amp/cm ²)	E_o (Volts) ^a	α
1	CP	30	82	1.33E-03	0.316	0.73
2	CP	50	83	3.94E-06	0.244	0.77
3	CP	75	66	3.31E-06	0.139	1.04
3dup	CP	75	155	3.77E-05	-0.504	0.44
4	AP	30	182	1.93E-04	1.009	0.33
5	AP	50	143	3.83E-04	1.001	0.45
6	AP	75	154	7.60E-04	1.002	0.45
6dup	AP	75	172	5.07E-07	0.654	0.40
With HM Sludge Simulant diluted to 20:1 by solution						
7	CP	30	88	1.76E-06	0.251	0.68
8	CP	50	58	5.67E-07	0.191	1.10
9	CP	75	120	6.91E-06	0.165	0.57
9dup	CP	75	74	1.15E-06	0.215	0.93
10	AP	30	61	9.98E-07	1.070	0.98
11	AP	50	97	1.62E-06	1.053	0.66
12	AP	75	65	2.84E-07	1.110	1.06

5 Conclusions

The testing presented in this report examined the corrosion of A285 carbon steel and 304L stainless steel exposed to two proposed chemical cleaning solution composed of 0.18M nitric acid and 0.5 sodium permanganate (acidic permanganate) and 10M sodium hydroxide and 0.5 sodium permanganate (caustic permanganate). These solutions have been proposed as a chemical cleaning solution for the retrieval of actinides in the sludge in the waste tanks and were tested with both HM and PUREX sludge simulants.

The corrosion rates determined from passive coupons testing for the A285 carbon steel exposed to the PUREX sludge was found to be as high as 70 MPY at 25°C and 125 MPY at 50°C in the acidic permanganate. Previous testing⁶, show the corrosion rate determined by electrochemical methods to be about 3 MPY at room temperature (about 22°C). The passive coupons displayed signs of general corrosion and pitting corrosion with pits as wide as 2-6 mm and about 1mm deep. There were only 1 or 2 major pits on the coupons that have a surface area of 5.42 in². The large pits could undoubtedly be responsible for the biased corrosion rates in the passive coupon tests. The presence of localized corrosion agrees with the electrochemical data that displayed a positive hysteresis. The corrosion rate was observed to decrease of the testing period at 50°C and remained constant at 25°C.

The corrosion behavior of 304L stainless steel in the cleaning solutions with the sludge was also studied using passive coupon testing at 25°C and 50°C. The corrosion rates were very low in both the acid and caustic permanganate with the highest rate being 0.037 MPY. The coupons that were exposed to the caustic permanganate solution turned a golden straw color during the testing. SEM/EDX observations showed that these coupons had deposits of aluminum and manganese. The coupons did not have any observable signs of pitting.

Electrochemical tests were conducted on 304L stainless steel with cleaning solutions contacted with the HM sludge at a 20:1 ratio at temperatures of 30°C, 50°C, and 75°C. The electrochemical tests were used to determine the corrosion rate, propensity for localized corrosion, and the likelihood of hydrogen evolution. The highest corrosion rates were around 35 MPY at 75°C in the caustic permanganate solution which was much higher than the corrosion rates for the passive coupon tests. However, the electrochemical tests can over estimate corrosion rates since the measurement is of the instantaneous measurement. In the passive coupon tests, the coupons changed color resulting in metal deposited on to the surface which may have passivated the steel against corrosion. However, with the sludge present there could be other reactions taking place at the surface of the electrode that contribute to the current, but are not directly related to the oxidation of the stainless steel. The electrochemical tests did not indicate hydrogen evolution was likely in either the caustic or acidic permanganate due to the high noble potential of the stainless steel in the environments.





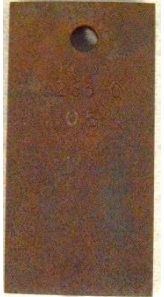




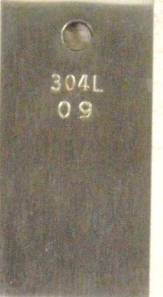
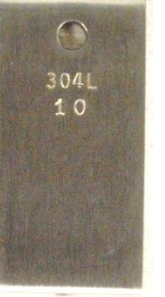





6 References

1. Martin., K.B., "Evaluation of the Impact of Removing Corrosion Controls During Waste Tank Closure Activities", C-ESR-F-00041, Rev. 5, March 2013.
2. Office of Tank Waste & Nuclear Materials (EM-20), Work Authorization/Task Change Request HQTD1001, Waste Retrieval and Closure Technologies, February 2014.
3. Suduth, C., J. Vitalli, M. Keefer, "Evaluation of Sludge Heel Dissolution Efficiency with Oxalic Acid Cleaning at Savannah River Site", Waste Management 20 Conference, Paper # 14205, March 2014.
4. Isom, S. T., A. G. Garrison. "Evaluation of the Impact of Oxalate Formation from Bulk Oxalic Acid Cleaning (BOAC) on the Concentration, Storage, and Transfer Facilities (CSTF) and Downstream Facilities", X-ESR-G-00037, Rev. 0, March 2014.
5. King, W. D., M. S. Hay, "Alternative Enhanced Chemical Cleaning: Basic Studies Results FY09", SRNL-STI-2009-00791, Rev. 0, February 2010.
6. Wyrwas, R. B., "Annual Report, Spring 2015: Alternative Chemical Cleaning Methods for High Level Waste Tanks – Corrosion Test Results," SRNL-STI-2015-00302, Rev. 0, May 2015.
7. King, W. D., M. S. Hay, "Alternative Enhanced Chemical Cleaning: Basic Studies Results FY10", SRNL-STI-2010-00541, Rev. 0, January 2011.
8. King, W. D., M. S. Hay, "Real Waste Testing Recommendations for Sludge Heel Dissolution in Oxalic Acid", L3100-2010-00203, Rev. 0, September 2010.
9. Wiersma, B. J., "Alternative and Enhanced Chemical Cleaning: Corrosion Studies Results FY10", SRNL-STI-2010-00555, Rev. 0, September 2010.; Wiersma, B. J., "Treatment Tank Corrosion Studies for the Enhanced Chemical Cleaning Process", SRNL-STI-2010-00535, Rev.1, August 2011.
10. Rudisill, T. S., M. C. Thompson, "Enhanced Chemical Cleaning of SRS Wastes to Improve Actinide Solubility", SRNL-STI-2011-00521, Rev. 0, September 2011.













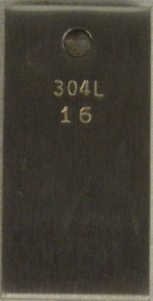



11. Eibling, R. E. "Development of Hazardous Sludge Simulants for Enhanced Chemical Cleaning Tests", SRNL-STI-2010-00170, Rev. 0, April 2010.
12. Wyrwas, R. B., "SRNL Task Technical and Quality Assurance Plan for the Alternative Chemical Cleaning of Radioactive High Level Waste Tanks: Corrosion Testing", SRNL-RP-2015-00808 Rev.0, September 2015.
13. ASTM G 59-97, "Standard Test Method for Conducting Potentiodynamic Polarization Resistance Measurements," ASTM International, West Conshohocken, PA, 2014.
14. F. Mansfeld, "The Polarization Resistance Technique", in Advances in Corrosion Science and Technology, Vol.6, eds. M. G. Fontana and R. W. Staehle, Plenum Press, New York, NY, 1976, p. 163.
15. M. Stern and A. L. Geary, J. Electrochemical Society, Vol. 104, No. 1, pp. 56-63, 1957.
16. H. H. Uhlig, Corrosion and Corrosion Control, 2nd Edition, John Wiley and Sons, NY, NY, 1971.
17. ASTM G 1-03, "Standard Practice for Preparing, Cleaning, and Evaluating Corrosion Test Specimens," ASTM International, West Conshohocken, PA, 2011.

Appendix A
Photographs of Weight Loss Coupons Post-Test Cleaning

50°C Testing

Caustic Permanganate	1 Week	3 Weeks	4 Weeks	Last Week
				
Coupon #	SS 07 (A1)	SS 05 (A3)	SS 06 (A4)	SS 25 (B)
Caustic Permanganate				
				
Coupon #	CS 05 (A1)	CS 07 (A3)	CS 06 (A4)	CS 21 (B)
Acid Permanganate				
				
Coupon #	SS 08 (A1)	SS 09 (A3)	SS 10 (A4)	SS 24 (B)
Acid Permanganate				
				
Coupon #	CS 24 (A1)	CS 25 (A3)	CS 22 (B)	CS 23 (A4)

25°C Testing

Caustic Permanganate	1 Week	3 Weeks	4 Weeks	Last Week
				
Coupon #	CS 10 (A1)	CS 08 (A3)	CS 09 (A4)	CS 12 (B)
Caustic Permanganate				
				
Coupon #	SS 12 (A1)	SS 13 (A3)	SS 11 (A3)	SS 14 (B)
Acid Permanganate				
				
Coupon #	CS 17 (A1)	CS 15 (A3)	CS 16 (A4)	CS 11 (B)
Acid Permanganate				
				
Coupon #	SS 16 (A1)	SS 18 (A3)	SS 17 (A4)	SS 15 (B)

Appendix B
CPP Data

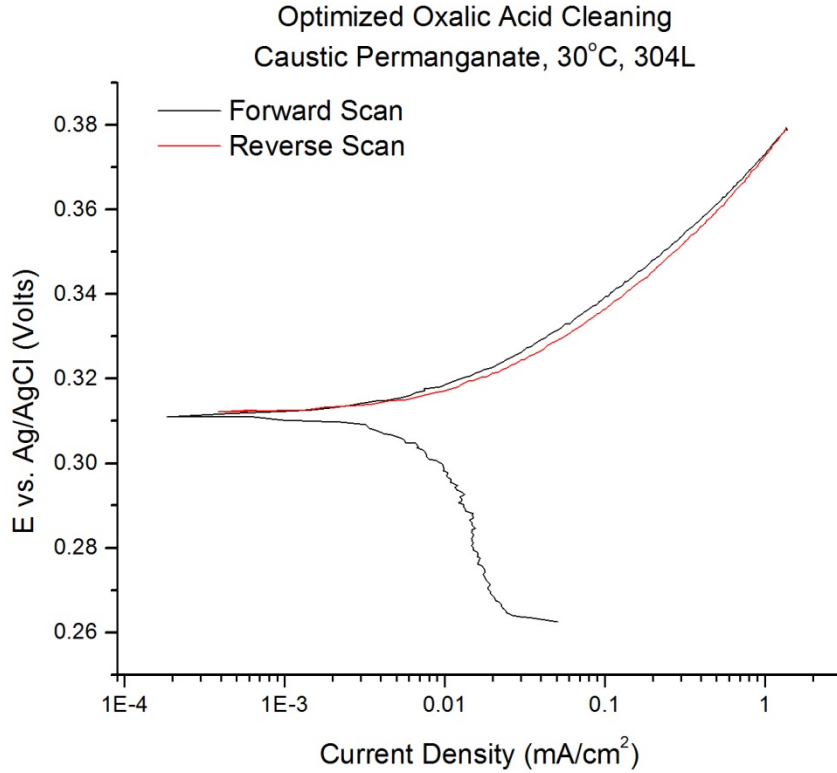


Figure B-6-1. Cyclic Potentiodynamic Polarization Curve of Caustic Permanganate at 30°C.

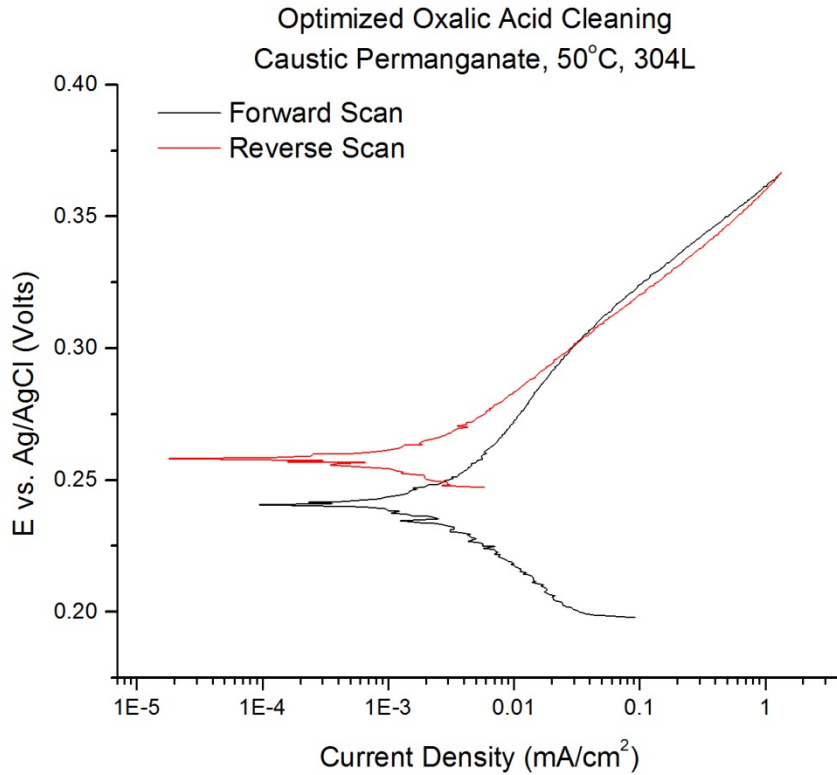


Figure B-6-2 Cyclic Potentiodynamic Polarization Curve of Caustic Permanganate at 50°C.

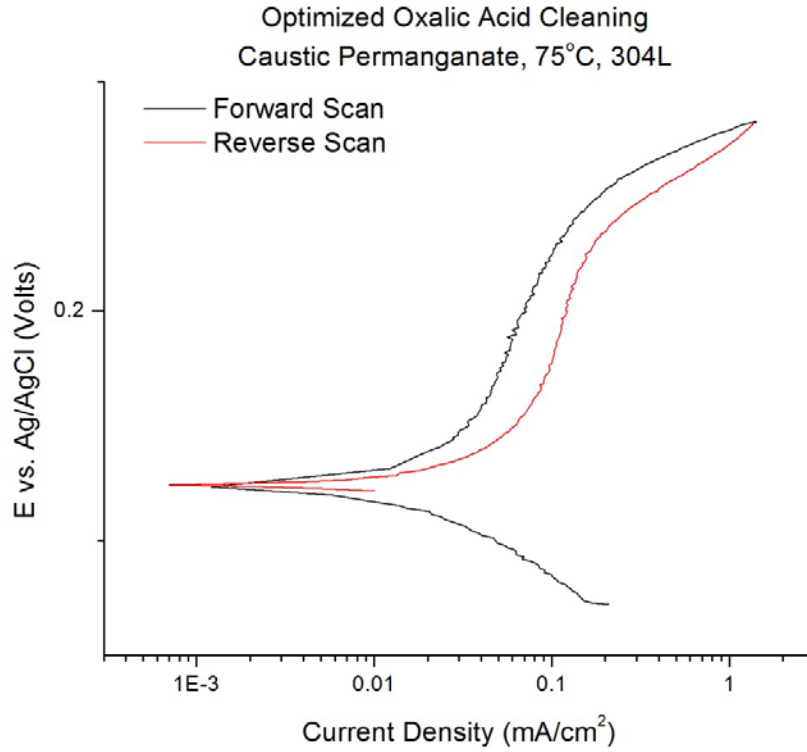


Figure B-6-3. Cyclic Potentiodynamic Polarization Curve of Caustic Permanganate at 75°C.

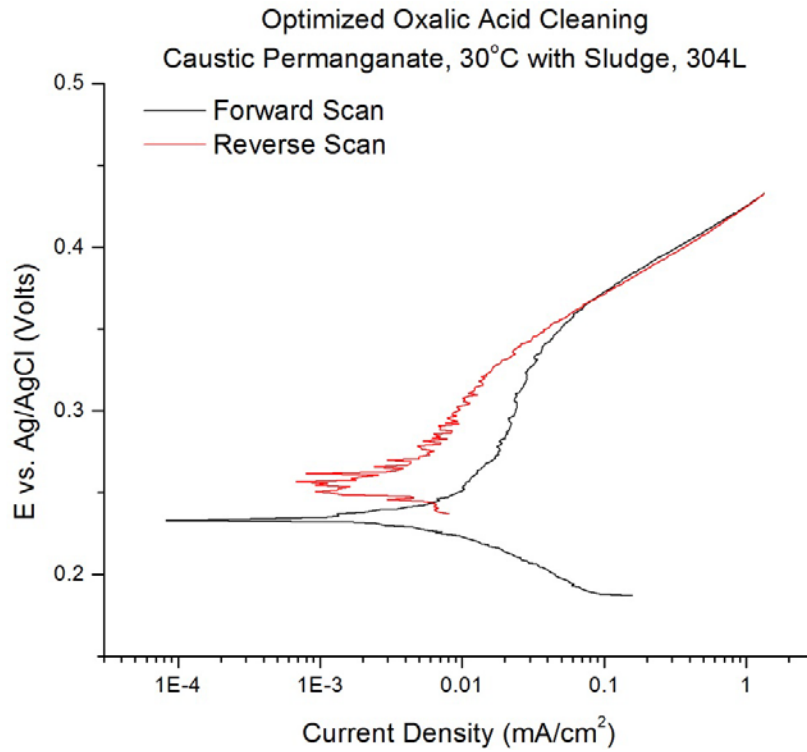


Figure B-6-4. Cyclic Potentiodynamic Polarization Curve of Caustic Permanganate with Sludge at 30°C.

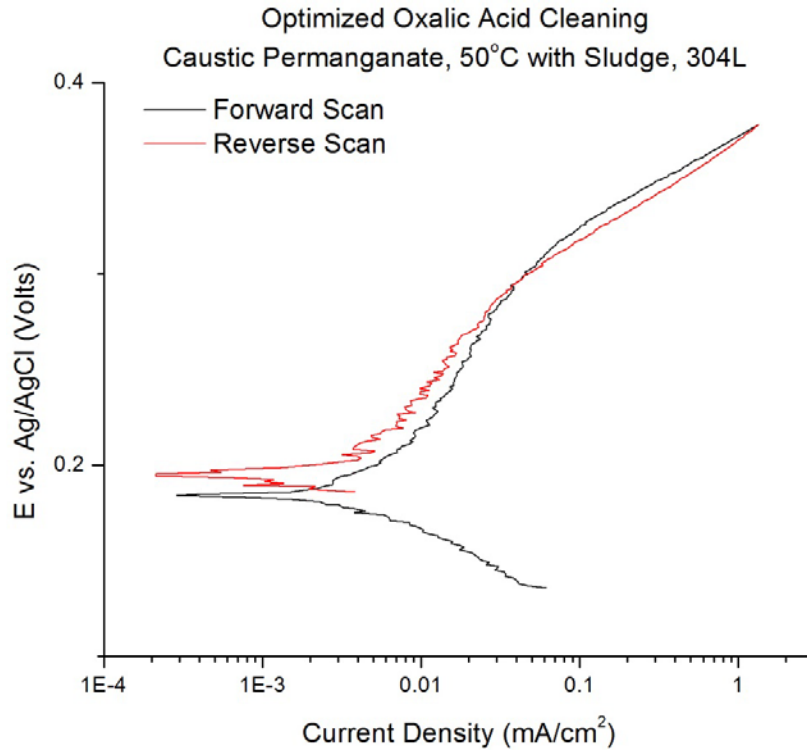


Figure B-6-5. Cyclic Potentiodynamic Polarization Curve of Caustic Permanganate with Sludge at 50°C.

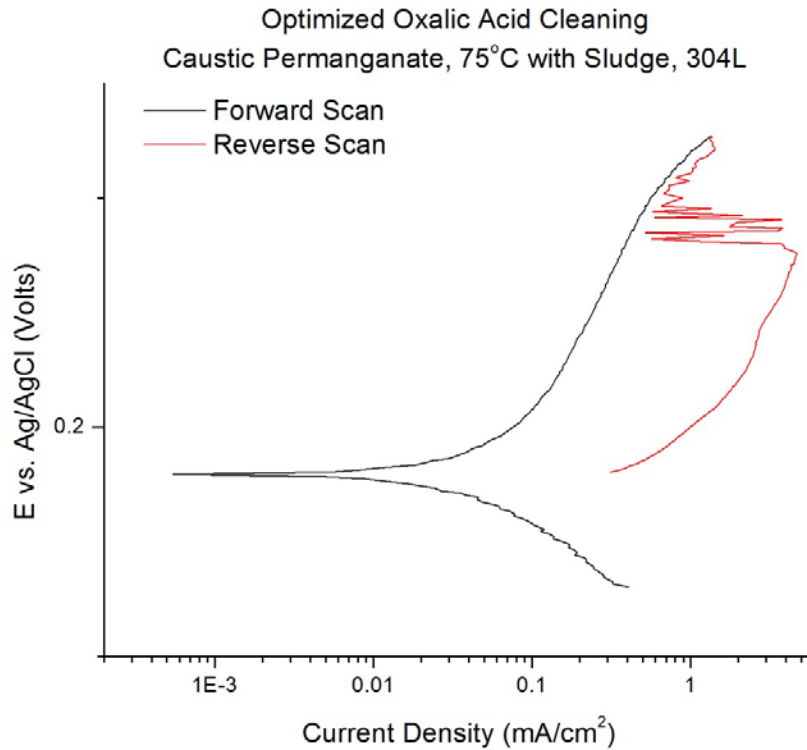


Figure B-6-6. Cyclic Potentiodynamic Polarization Curve of Caustic Permanganate with Sludge at 75°C.

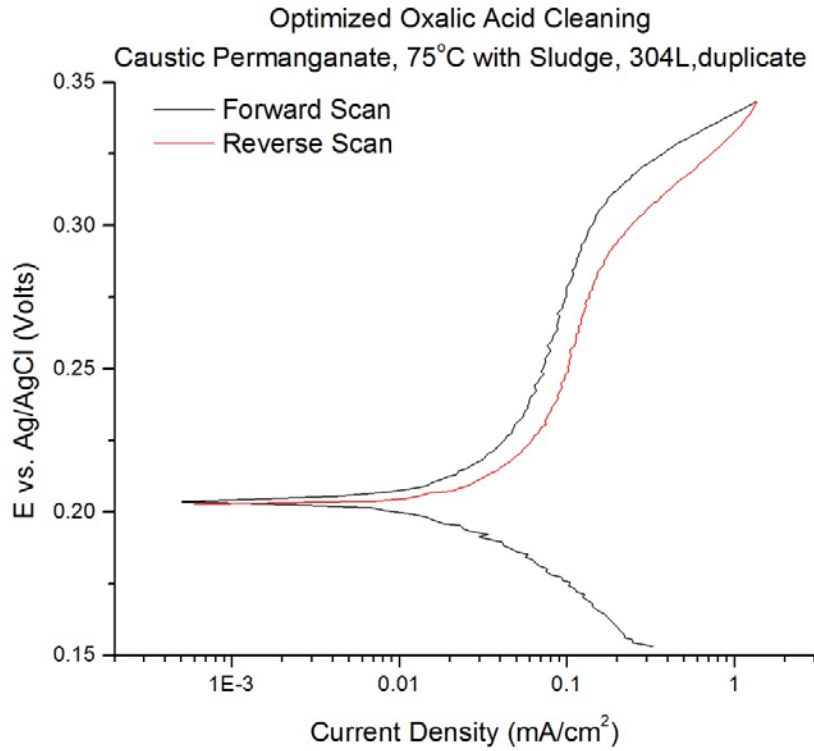


Figure B-6-7. Cyclic Potentiodynamic Polarization Curve of Caustic Permanganate with Sludge at 75°C.

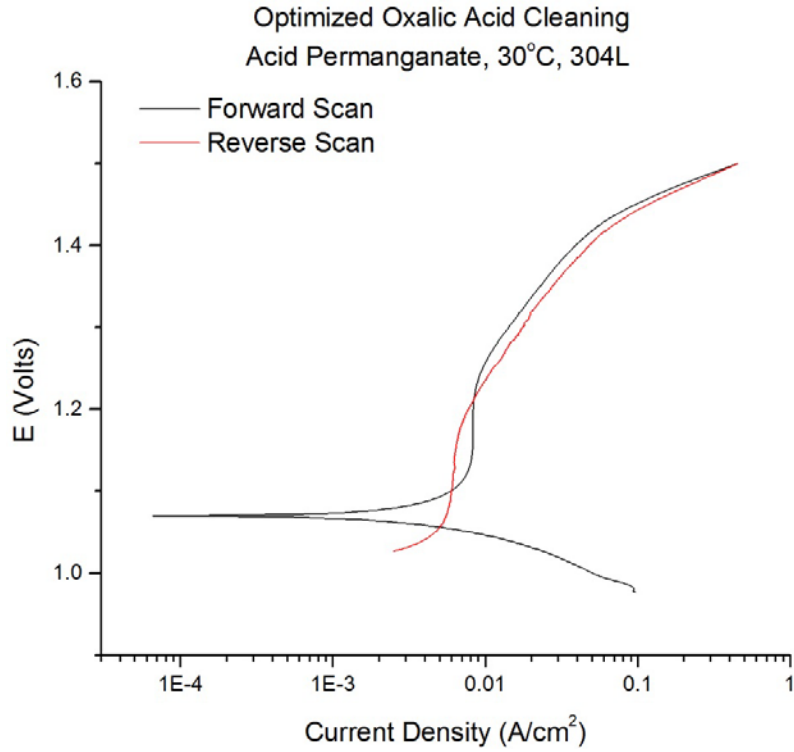


Figure B-6-8. Cyclic Potentiodynamic Polarization Curve of Acidic Permanganate at 30°C.

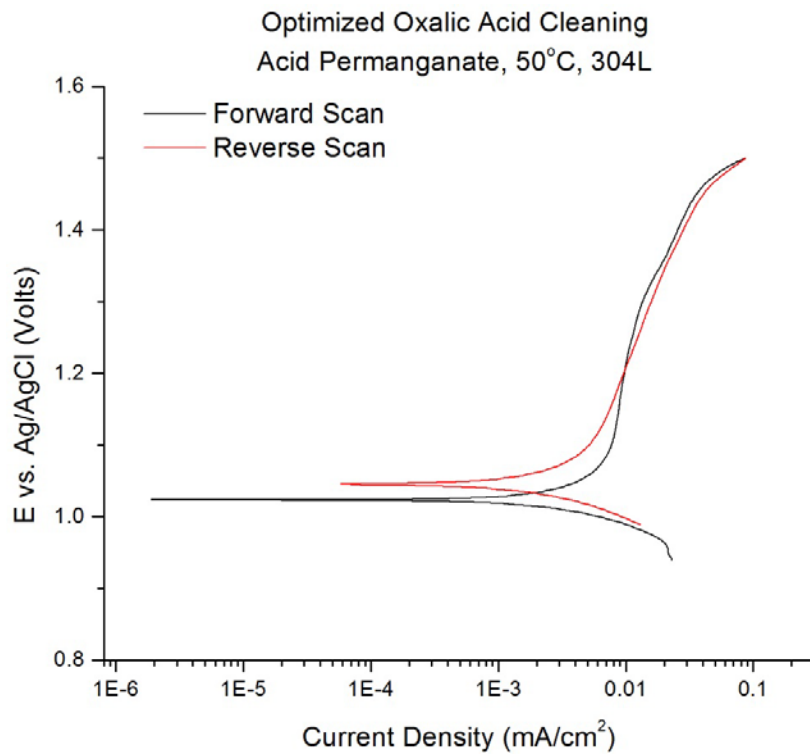


Figure B-6-9. Cyclic Potentiodynamic Polarization Curve of Acidic Permanganate at 50°C.

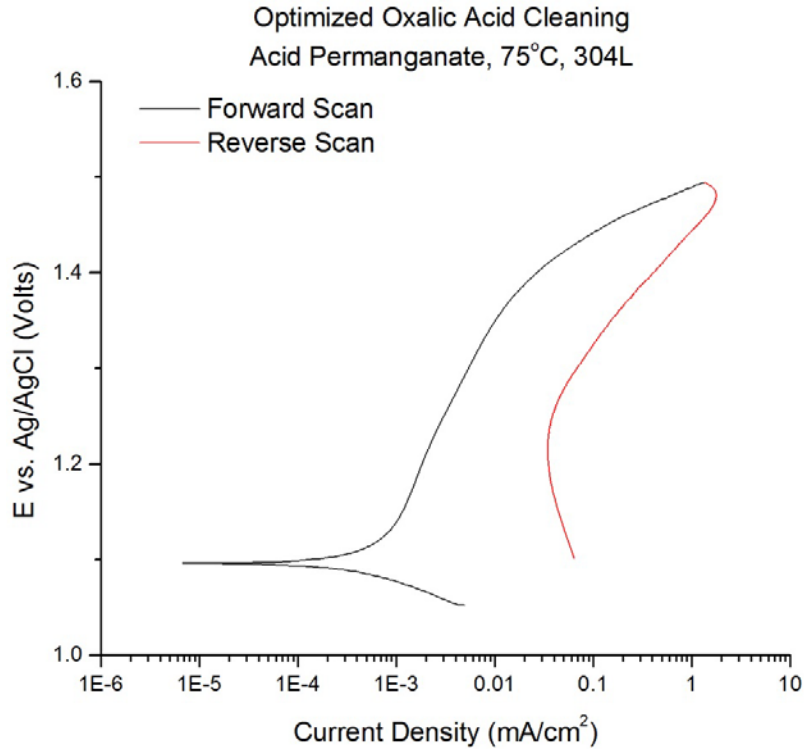


Figure B-6-10. Cyclic Potentiodynamic Polarization Curve of Acidic Permanganate at 75°C.

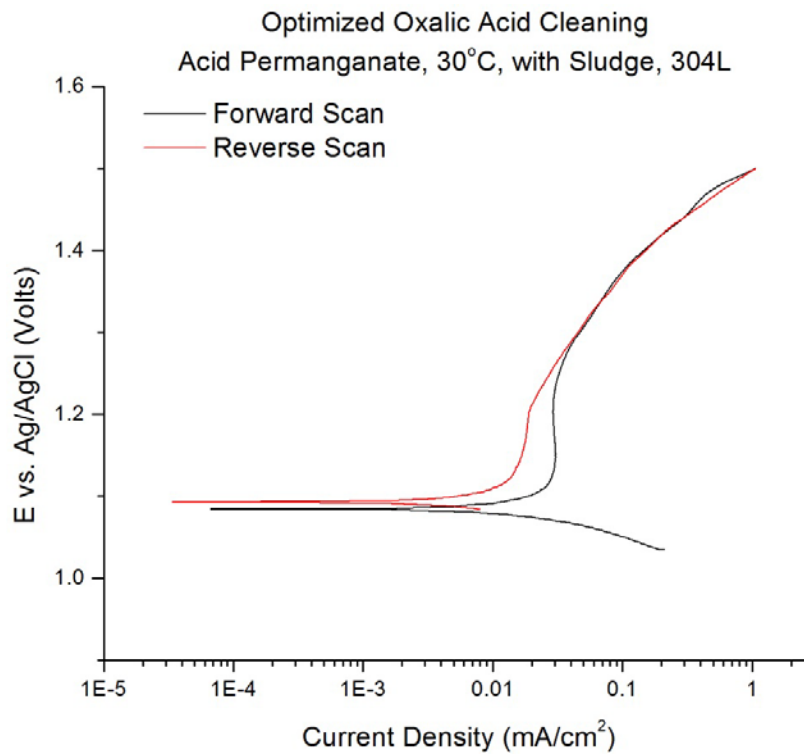


Figure B-6-11. Cyclic Potentiodynamic Polarization Curve of Acidic Permanganate with Sludge at 30°C.

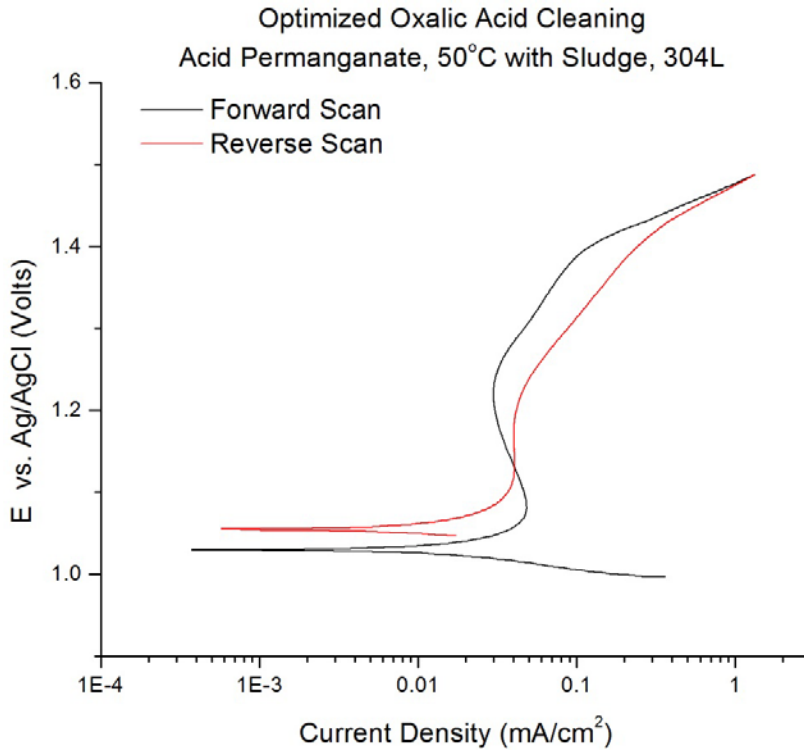


Figure B-6-12. Cyclic Potentiodynamic Polarization Curve of Acidic Permanganate with Sludge at 50°C.

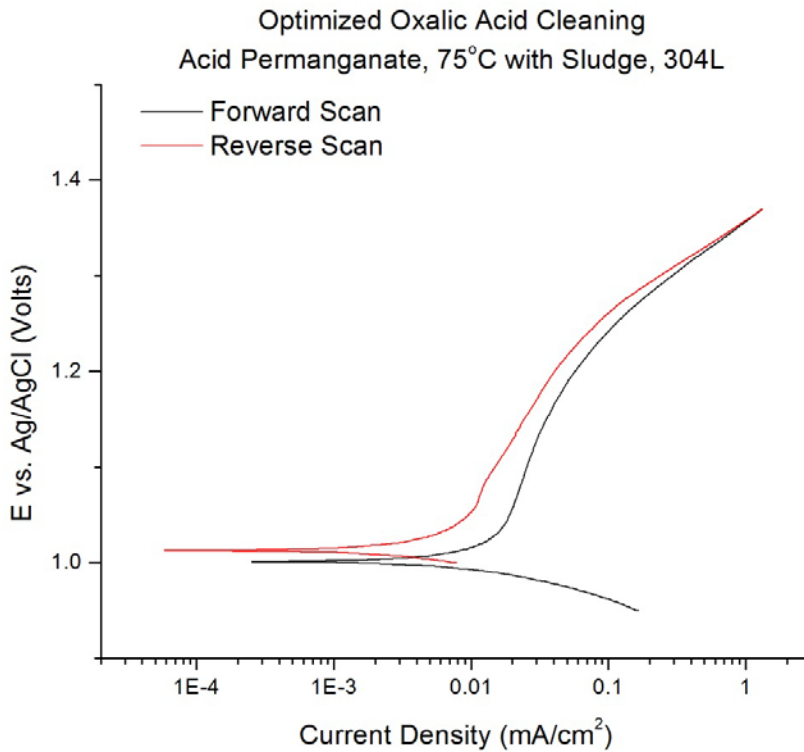


Figure B-6-13. Cyclic Potentiodynamic Polarization Curve of Acidic Permanganate with Sludge at 75°C.

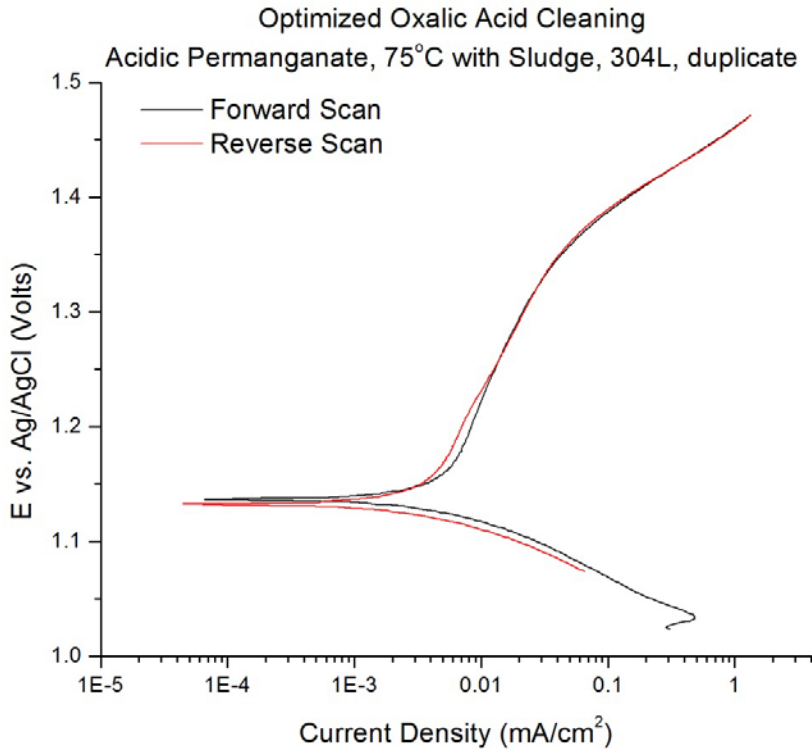


Figure B-6-14. Cyclic Potentiodynamic Polarization Curve of Acidic Permanganate with Sludge at 75°C.